Computer Vision — CVWW'03, Ondřej Drbohlav (ed.)
Valtice, Czech Republic, February 3–6, 2003
Czech Pattern Recognition Society

Rigid multi-modality registration of medical images using point similarity measures

Peter Rogelj and Stanislav Kovačič

Faculty of Electrical Engineering, University of Ljubljana,
Tržaška 25, SI-1000 Ljubljana, Slovenia
peter.rogelj@fe.uni-lj.si, stanislav.kovacic@fe.uni-lj.si

Abstract *Rigid registration is usually performed as an optimization procedure that searches for an image transformation that gives best similarity between the registered images. Similarity is used as a measure of image correspondence. In this work we present an implementation of rigid multi-modality registration based on point similarity measures, which were developed for non-rigid registration tasks. The system was evaluated by The retrospective registration evaluation project. The obtained results prove that point similarity measures are also suitable for various rigid registration tasks.*

1 Introduction

The aim of rigid image registration is to determine a spatial transformation that best aligns source image B to the target image A. The transformation consists of six parameters, which represent image translation and rotation. Image registration procedures are based on the assumption that higher similarity between the images corresponds to more correct image alignment. This enables the registration to be preformed as an optimization of transformation parameters using image similarity as the optimization criterion. However, the presumption is not necessarily correct. Function of similarity is not smooth according to the image misalignment, it includes local extrema, and furthermore, a global extremum may not appear exactly at the best image alignment. To overcome these problems several optimization procedures [4] and similarity measures [6, 2] have been introduced.

Our implementation of rigid registration algorithm is based on point similarity measures, which were developed for solving high-dimensional non-rigid registration tasks. In addition to their multi-modality capabilities they enable measuring the similarity of arbitrarily small image regions, and provide good local sensitivity for all tissue types irrespective of their amount. The major difficulty in further developments of non-rigid registration techniques is that at present an objective evaluation scheme is not available. On the other hand, thanks to The retrospective registration evaluation project [1], rigid registration systems can be objectively compared with the reference prospective registration technique. This motivated us to implement a rigid registration system using our point similarity measures, which allowed us to show their performance using standard evaluation approach.

2 Point similarity measures

Point similarity measures [7] were developed for non-rigid registration tasks, where extreme locality is required to detect detailed image discrepancies. They are based on information derived from the whole images, but enable measuring similarity of arbitrarily small image regions, including similarity of individual image points.

Similarity measurement using point similarity measures is a two step process. In the first step similarity function $S(\mathbf{i})$ is estimated, and in the second similarity $S(v)$ of certain image point pair v is determined. Similarity function defines the similarity of all possible intensity pairs $\mathbf{i} = (i_A, i_B)$, where i_A and i_B are the intensities of target and source image respectively. The estimation of similarity function is based on joint intensity distribution $p(\mathbf{i})$, which can be obtained from the images by normalizing joint intensity histogram or by Parzen window estimation [5].

The joint intensity distribution obtained from the images changes according to the quality of image alignment. Only the joint intensity distribution of correctly aligned images represents the correct image intensity dependence. As this distribution is not known until the images are correctly registered, the estimation of similarity function is based on the available joint intensity distribution $p(\mathbf{i})$.

Several point similarity measures exist. They differ only in the way how similarity function $S(\mathbf{i})$ is estimated from the joint distribution $p(\mathbf{i})$. The one, which we use for multi-modality rigid registration, is the following:

$$\begin{aligned} S(\mathbf{i}) &= \log(p(i_A|i_B) \cdot p(i_B|i_A)) = \\ &= \log \frac{p(\mathbf{i})^2}{p(i_A) \cdot p(i_B)}, \end{aligned} \tag{1}$$

where $p(i_A|i_B)$ and $p(i_B|i_A)$ denote conditional intensity distributions, while $p(i_A)$ and $p(i_B)$ denote marginal intensity distributions. $S(\mathbf{i})$ is better estimated when intensity distributions are obtained at better image alignment. If the alignment is very poor, $S(\mathbf{i})$ significantly differs from the correct image intensity dependence and such registration may not be successful.

The second step in similarity measurement using point similarity measures is determination of similarity $S(v)$ for certain image point or voxel v. It can be determined directly from the similarity function $S(\mathbf{i})$,

$$S(v) = S(\mathbf{i}(v)) \tag{2}$$

where $\mathbf{i}(v) = (i_A(v), i_B(v))$ denotes an intensity pair at point v. When the source image (B) is being transformed, $\mathbf{i}(v)$ also depends on the transformation $\mathbf{T}$, such that

$$S(v, \mathbf{T}) = S(\mathbf{i}(v, \mathbf{T})). \tag{3}$$

Similarity of the whole images, needed for rigid registration, can be computed by averaging point similarities over all image voxels,

$$S_G(\mathbf{T}) = \overline{S(v, \mathbf{T})}. \tag{4}$$

Note that similarities $S_G(\mathbf{T})$ or $S(v, \mathbf{T})$ obtained at different transformations $\mathbf{T}$ may be compared only if they are based on the same similarity function $S(\mathbf{i})$.

3 Rigid registration approach

Following the standard approach, the registration is implemented as an optimization procedure that maximizes a global image similarity $S_G(\mathbf{T})$, see Figure 1.

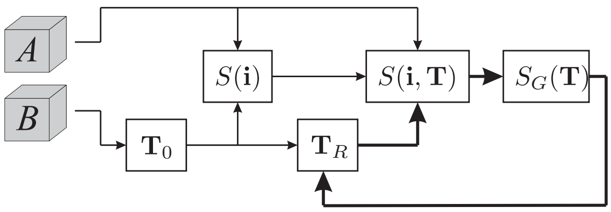

Figure 1: Rigid registration based on point similarity measures. The registration consists of two steps: estimation of the similarity function $S(\mathbf{i})$ and an optimization procedure that optimizes transformation T_R. The optimization loop is presented by thicker line.

In contrast to standard approaches, registration based on point similarity measures consists of two steps. In the first step the similarity function $S(\mathbf{i})$ is estimated from the joint intensity distribution $p(\mathbf{i})$, using Eq. (1). Here, the joint distribution $p(\mathbf{i})$ is obtained from the images A and B at some initial transformation $\mathbf{T}_0$, using partial volume interpolation [3]. The transformation $\mathbf{T}_0$ is used to obtain adequate initial image overlap, required by point similarity measures, or to possibly continue the registration at transformation obtained in previous registration steps.

In the second registration step, better image alignment is searched using Powell optimization algorithm. The overall transformation $\mathbf{T}$ is divided into two actual transformations, the initial one $\mathbf{T}_0$, and the additional one $\mathbf{T}_R$ that is initially set to identity and is changed by the optimization procedure. The optimization criterion is a global image similarity $S_G(\mathbf{T})$ computed from point similarities $S(v, \mathbf{T})$ of all source image voxels v, see Eq. (4). When optimization converges, the overall transformation $\mathbf{T}$ that rigidly registers the images is computed:

$$\mathbf{T} = \mathbf{T}_R \cdot \mathbf{T}_0. \tag{5}$$

Because of possibly different voxel sizes of images A and B, and the transformation of image B, point similarities $S(v, \mathbf{T})$ must be determined using interpolation. A commonly used approach is to interpolate intensities of one image in order to obtain intensity pairs $\mathbf{i}(v)$, used for measuring the similarity $S(v, \mathbf{T}) = S(\mathbf{i}(v, \mathbf{T}))$. This is not an appropriate method for estimating multi-modality point similarities. Multi-modality intensity dependencies are not linear and therefore they should not be modelled by linear intensity models. Intensities obtained with linear intensity interpolation could introduce additional interpolation artifacts. We solve this problem by using interpolation of similarities instead of intensities. Specifically, a point similarity $S(v)$ is determined by interpolating similarities $S(i_{Ak}(v), i_B(v))$, where i_{Ak} denotes intensities of voxels in image A, surrounding the point v. This approach eliminates all the interpolation artifacts that commonly appear when using other multi-modality similarity measures, which may enable higher registration precision.

4 Multiresolution implementation

A multiresolution approach is used to avoid local minima, improve robustness and reduce computational complexity. The registration is performed in K resolutions ($k = 0..K-1$), where $k = 0$ denotes the original image resolution. Subsampled images $A(k)$ and $B(k)$ are obtained by using $3 \times 3 \times 3$ median filtering to remove high image frequencies. Median filtering is used as a replacement to the commonly used linear filtering, which is due to the presumed linear intensity dependence not suitable for multi-modality registration.

Each resolution level consists of N steps of registration, see Figure 2, where each of the steps is performed as described in Section 3, Figure 1.

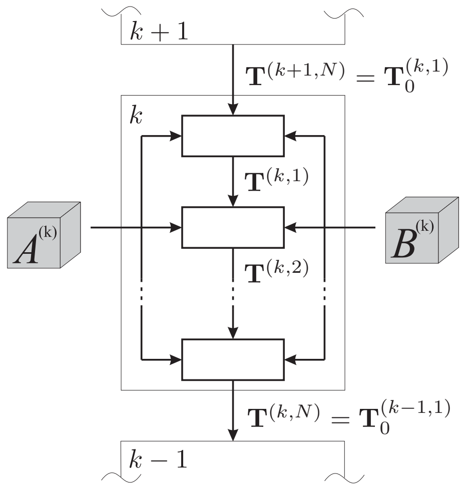

Figure 2: Scheme of multiresolution implementation. Registration is performed in K resolutions ($k = 1..K$), each of them consisting of N registration steps.

The first step ($n = 1$) in the lowest resolution ($k = K-1$) starts with initial image correspondence and thus an iden-

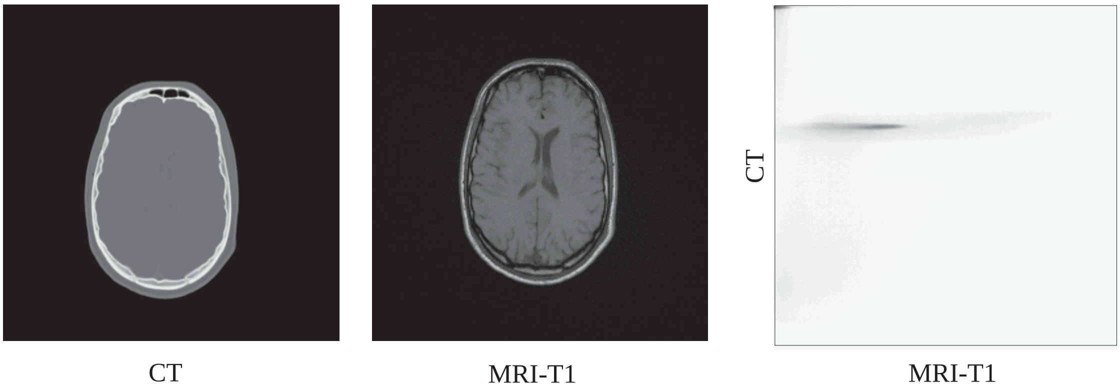

Figure 3: Sample images for CT to MRI-T1 registration and corresponding joint intensity distribution of registered images (darker color corresponds to higher probability).

Table 1: Registration errors for registering CT images to MRI-T1 images, for 10 anatomical points (VOI 1-10) and all 16 available patients.

	VOI 1	VOI 2	VOI 3	VOI 4	VOI 5	VOI 6	VOI 7	VOI 8	VOI 9	VOI 10
pt001	1.318411	1.414050	2.067559	2.050089	1.539542	1.768205	1.951642	2.251120	1.451773	1.731921
pt002	———	1.361990	0.922660	0.659307	0.900857	0.512490	0.483710	1.693390	2.055826	1.921117
pt003	———	1.353354	1.572636	2.027756	1.402924	2.033294	1.336319	2.040582	1.560603	1.406557
pt004	———	———	———	———	———	1.961030	2.362611	1.749931	3.096772	3.112965
pt005	2.289893	2.194829	1.687327	1.396784	1.912644	1.477669	1.767082	2.069966	2.456541	2.473416
pt006	1.015653	1.037236	1.778054	2.088307	1.218297	1.646424	1.425881	1.834135	1.144019	1.278415
pt007	———	1.010118	1.003693	1.099953	1.000694	1.076686	1.021505	1.144803	1.015022	1.074432
pt101	2.214423	2.149883	2.050327	2.163085	2.118768	2.161599	2.022113	1.780373	2.098204	2.085105
pt102	1.362441	1.376753	2.389910	1.554298	1.580498	1.010325	2.415886	2.102256	1.308687	1.701420
pt103	2.597908	2.425481	2.369233	2.718541	2.480992	2.479410	2.021983	1.202205	2.244241	2.285358
pt104	1.559718	1.428977	1.343269	1.500759	1.491924	1.307704	1.097213	1.045764	1.617440	1.564693
pt105	2.355182	2.300441	2.360760	2.145938	2.283106	2.047241	2.451419	2.111519	2.220994	2.397404
pt106	1.822191	1.900953	2.066917	2.207116	1.915152	2.183549	1.879381	2.401565	2.055893	1.901160
pt107	2.504540	2.179510	2.085615	1.809047	1.802098	2.111907	3.040904	2.286672	1.897290	2.734406
pt108	1.422902	1.421461	1.451562	1.393379	1.422370	1.372511	1.469269	1.411851	1.406748	1.438731
pt109	1.621355	1.494555	1.463794	1.536585	1.541295	1.373264	1.296285	0.841338	1.660091	1.655860

mean = 1.76 mm, median = 1.76 mm, maximum = 3.11 mm

tity transformation $\mathbf{T}_0^{(K-1,1)} = \mathbf{I}$. The next step $(n+1)$ uses resulting transformation of previous step $\mathbf{T}^{(k,n)}$ as initial transformation $\mathbf{T}_0^{(k,n+1)}$,

$$\mathbf{T}_0^{(k,n+1)} = \mathbf{T}^{(k,n)} \quad ; \quad n = 1..(N-1). \tag{6}$$

or when changing the resolution level,

$$\mathbf{T}_0^{(k,1)} = \mathbf{T}^{(k+1,N)}. \tag{7}$$

Specifically, we use four resolution levels ($K = 4$), where each level consists of three registration steps ($N = 3$).

5 Results

The system was evaluated by ”The retrospective registration evaluation project” [8], which was designed to compare retrospective CT-MRI and PET-MRI registration techniques used by a number of groups. It involves the use of an FTP image database to allow the downloading of image volumes on which the registrations are to be performed. The idea is that the collaborating groups perform registrations on the image volumes, using their own retrospective techniques, and the group at Vanderbilt University evaluates the accuracy of these transformations by means of their own prospective, marker-based technique.

The image database includes images of 18 subjects, marked pt001-pt009 and pt101-pt109. The evaluation of registration accuracy was obtained by measuring registration errors for 10 points in brain anatomy marked as VOI1-VOI10. From all the results (for all points in all registered images) mean, median and maximum error is computed.

5.1 CT to MRI registration

Registration of CT images to MRI-T1 images was performed using 16 available CT-MRI image pairs (CT images for patients pt008 and pt009 are missing). Images have different voxel sizes: images of subjects pt001-pt009 have $0.65 \times 0.56 \times 4$ mm voxel size for CT images and $1.25 \times 1.25 \times 4$ mm for MRI images, while subjects pt101-pt109 have $0.45 \times 0.45 \times 3$ mm voxel size for CT images

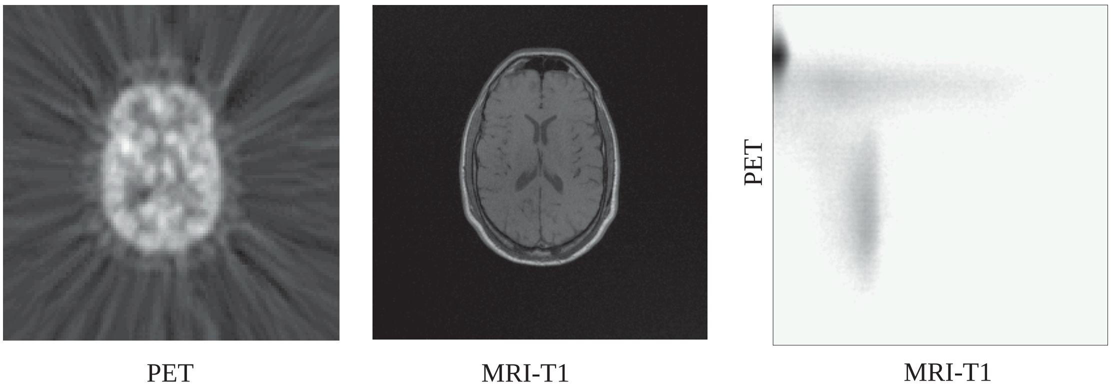

Figure 4: Sample images for PET to MRI-T1 registration and corresponding joint intensity distribution of registered images (darker color corresponds to higher probability).

Table 2: Registration errors for registering PET images to MRI-T1 images, for 10 anatomical points (VOI 1-10) and all 7 available patients.

	VOI 1	VOI 2	VOI 3	VOI 4	VOI 5	VOI 6	VOI 7	VOI 8	VOI 9	VOI 10
pt001	0.974484	0.750237	1.740664	2.169446	0.629607	1.211050	0.799778	1.556204	1.089950	1.224679
pt002	———	1.699095	2.596562	2.353774	1.922822	1.812047	2.206658	1.043201	1.239837	1.479047
pt005	1.877124	1.815363	2.998484	2.266538	1.613928	1.537461	2.743053	2.265476	2.710502	2.333102
pt006	9.732683	9.593348	8.936985	6.138780	8.863224	6.246626	9.949534	9.149637	9.497526	11.219258
pt007	———	3.416825	5.472465	4.826450	3.864866	3.477531	4.631028	1.619964	2.593110	3.184805
pt008	———	3.537144	3.278741	3.701926	3.469292	3.755874	3.007465	3.104460	3.787213	3.452140
pt009	———	———	———	———	———	3.509255	4.634637	3.127904	3.072052	3.537593

mean = 3.58 mm, median = 3.00 mm, maximum = 11.22 mm

and $0.86 \times 0.86 \times 3$ mm for MRI images. Sample images and corresponding joint intensity distribution are shown in Figure 3.

The results of registering CT images to MRI-T1 images are tabulated in Table 1. All the registrations were successful, resulting in overall mean error 1.76 mm, median error 1.76 mm and maximal error 3.11 mm. Results for subjects pt101-pt109, where images have smaller voxel sizes, were in general not better than the results for subjects pt001-pt107, as one may expect. This indicates that the source of registration errors is not in the discrete nature of data, but in the images themselves. Note that imaged anatomies are not absolutely rigid and furthermore, MRI images may be deformed due to the magnetic field inhomogeneity, caused by presence of the subject.

5.2 PET to MRI registration

Registration of PET images to MRI-T1 images was performed using 7 available CT-MRI image pairs (patients pt001-pt009, excluding subjects pt003 and pt004 where PET images were missing). The voxel size for PET images is $2.6 \times 2.6 \times 8$ mm, while the voxel size for corresponding MRI-T1 images is $1.25 \times 1.25 \times 4$ mm. Sample images and corresponding joint intensity distribution are shown in Figure 4.

The results of registering PET images to MRI-T1 images are summarized in Table 2. One can observe that registration error for subject pt006 is high for all 10 anatomical points, which indicates that this registration was not successful. Including this subject, the overall mean error of 3.58 mm, median error of 3.00 mm and maximal error of 11.22 mm were obtained. Excluding the wrong registration, which could be detected by visual inspection of registered images, the mean error is 2.55 mm, median error is 2.47 and maximal error is 5.47 mm.

Errors for registration of PET images are in general higher than errors for registration of CT images. There are two reasons: first, the resolution of PET images is much lower than resolution of CT images, and second, PET is a functional imaging technique such that PET images comprise relatively low amount of anatomical information, required for matching with MRI images.

5.3 Comparison with other systems

We have compared the results of our method with results obtained by other research groups, see [1]. Until now, there are 43 participating groups, which contributed 113 sets of results. For the comparison we used only result sets with both CT-MRI T1 and PET-MRI T1 registration results, each of them obtained from registering at least 7 patients. Among these result sets we selected only the best one from each research group, and so we finally got 24 comparable result sets. We have compared them according to obtained mean registration errors. Comparison results are shown in Figure 5. Dashed lines correspond to mean values obtained by our rigid registration system, while other marks are used to

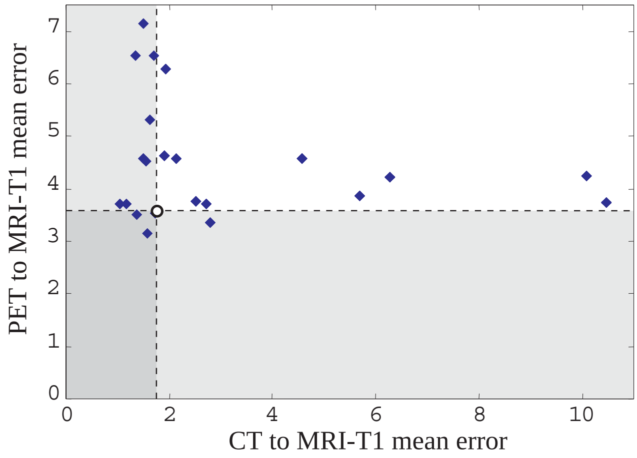

Figure 5: Graph showing mean errors of different rigid registration systems, for CT to MRI-T1 and PET to MRI-T1 registration. Dashed lines correspond to mean values obtained by our rigid registration system, while other marks are used to mark best results of other research groups. The darker shading correspond to a region with better results than ours for both types of registration.

mark best results of other research groups. The darker shading correspond to the region with better results for both types of registration while lighter shading corresponds to regions with better results in only one type of registration. Considering both types of registration, CT-MRI T1 and PET-T1, our system is one of the top six among 24 compared systems.

6 Conclusion

A multi-modality rigid registration approach based on point similarity measures was proposed. It was evaluated by The retrospective registration evaluation project and compared with best registration results of other research groups. The obtained results indicate that point similarity measures are comparable to mutual information measures in case of rigid registration, although they were designed for non-rigid registration tasks. As such they are suitable for solving various multi-modality rigid registration tasks.

Acknowledgement

The authors gratefully acknowledge the support of the Slovenian Ministry of Education, Science and Sport (research program 1538-517).

The images and evaluation results were provided as part of the ”Retrospective Image Registration Evaluation” project, National Institutes of Health, Principal Investigator: J. Michael Fitzpatrick, Vanderbilt University, Nashville, TN, project number 1 R0 CA89323.

References

[1] The retrospective registration evaluation project. *http://www.vuse.vanderbilt.edu/∼image/registration*.

[2] D. L. G. Hill and D. J. Hawkes. Across-modality registration using intensity-based cost functions. In I. Bankman, editor, *Handbook of Medical Image Processing*, pages 537–553. Academic Press, 1999.

[3] F. Maes, A. Collignon, D. Vandermeulen, G. MArchal, and P. Suetens. Multimodality image registration by maximization of mutual information. *IEEE Transactions on Medical Imaging*, 16(2):187–198, April 1997.

[4] F. Maes, D. Vandermeulen, and P. Suetens. Comparative evaluation of multiresolution optimization strategies for multimodality image registration by maximization of mutual information. *Medical Image Analysis*, 3(4):373–386, 1999.

[5] E. Parzen. On the estimation of probability density function. *Annual Mathematical Statistics*, 33:1065–1076, 1962.

[6] J. P. W. Pluim, J. B. A. Maintz, and M. A. Viergever. Image registration by maximization of combined mutual information and gradient information. *IEEE Transactions on Medical Imaging*, 19(8), 2000.

[7] P. Rogelj and S. Kovačič. Similarity measures for non-rigid registration. In M. Sonka and K. Hanson, editors, *Medical Imaging 2001: Image Processing*, volume 4322 of *Proc. SPIE*, pages 569–578. SPIE Press, Bellingham, WA, 2001.

[8] J. West, J. Fitzpatrick, M. Wang, B. Dawant, C. Maurer, R. Kessler, R. Maciunas, C. Barillot, D. Lemoine, A. Collignon, F. Maes, P. Suetens, D. Vandermeulen, P. van den Elsen, S. Napel, T. Sumanaweera, B. Harkness, P. Hemler, D. Hill, D. Hawkes, C. Studholme, J. Maintz, M. Viergever, G. Malandain, X. Pennec, M. Noz, G. Maguire, M. Pollack, C. Pelizzari, R. Robb, and R. Hanson, D. Woods. Comparison and evaluation of retrospective intermodality image registration techniques. *Journal of Computer Assisted Tomography*, 21(4):554–566, 1997.